NOTES AND CORRESPONDENCE

A Dust Prediction System with TOMS Initialization

P. ALPERT, S. O. KRICHAK, M. TSIDULKO, H. SHAFIR, AND J. H. JOSEPH

Department of Geophysics and Planetary Sciences, Tel Aviv University, Tel Aviv, Israel

1 April 2001 and 14 March 2002

ABSTRACT

A dust prediction system, developed earlier at the University of Athens within the framework of the Mediterranean Dust Experiment (MEDUSE) project, was enhanced at Tel Aviv University to support the Israeli–American Mediterranean Israeli Dust Experiment (MEIDEX) project. These enhancements include development of a dust initialization approach using Total Ozone Mapping Spectrometer (TOMS) aerosol index (AI) data and improved specification of the dust sources. The skill of the model against the TOMS AI measurements was tested during two periods in March and June 2000 using four different scores. It is shown that the TOMS-based initialization has a significant positive impact on all the scores. For instance, the average distance between the predicted and TOMS-observed dust plumes drops from 350–485 to less than 200 km. Verification of model forecasts against surface dust measurements in Tel Aviv shows correlations of up to 0.69 based on 27 predictions, for both 24 and 48 h. One example of a narrow dust plume over Israel, successfully forecast with the current system, is presented. This event occurred in midsummer (4 July) when dust bursts are rare over the Eastern Mediterranean.

1. Introduction

a. History of development of the dust prediction system at Tel Aviv University

The real-time weather and dust predictions at Tel Aviv University (TAU) are based on the National Centers for Environmental Prediction (NCEP) objective analysis retrieving and assimilation system. The TAU dust prediction model has been developed at the University of Athens within the framework of the Mediterranean Dust Experiment (MEDUSE) project (Nickovic et al. 1997). The system is based on the NCEP Eta Model and includes a package for the dust uptake/transport/deposition processes. With the aid of the University of Athens group, the model was imported to Tel Aviv University in October 1998 (Krichak et al. 1999a,b).

The dust prediction system was put into semioperative use at Tel Aviv University in February 1999. Several modifications were made to the model at Tel Aviv University including development of a new dust initialization system using Total Ozone Mapping Spectrometer (TOMS) aerosol index data, better determination of the dust sources [employing Ginoux et al.'s (2001) method, developed at the National Aeronautics and Space Administration Goddard Space Flight Center (NASA GSFC)], and expansion of the forecast area to include the Atlantic Ocean. These improvements were undertaken in order to support the joint Israeli–American Mediterranean Dust Experiment (MEIDEX). In MEIDEX, an Israeli astronaut will study from space dust plumes over the Mediterranean and the Atlantic region. Efforts were made to forecast the location of the center of mass and the orientation of the central axis of a plume with an acceptable error of not more than 200 km. The modified model will be shown to allow the realization of this target. (The current main Web site for the publication of the dust prediction is the MEIDEX URL: http://www.tau.ac.il/geophysics/MEIDEX).

b. Other dust prediction systems

There are other dust prediction systems that operate over the region. Several of these including the TAU version are based on the model originally developed by Nickovic and Dobricic (1996). In addition different approaches also exist, including the following: the U.S. Naval Research Laboratory (NRL) Aerosol Analysis and Prediction System (NAAPS; http://www.nrlmry.navy.mil/) has a global model component that is a modified form of that developed by Christensen (1997) and runs a global prediction system for several aerosol types. Another system is the Malta

Corresponding author address: Dr. Pinhas Alpert, Dept. of Geophysics and Planetary Sciences, Tel Aviv University, Tel Aviv 69978, Israel.
E-mail: pinhas@cyclone.tau.ac.il

model, Dust Regional Atmospheric Model (DREAM; http://www.icod.org.mt/aerosol/dust/med/dld), which is run by the Euro-Mediterranean Centre on Insular Cloud Dynamics (ICoD). This is a regional prediction system based on a modification of the Eta Model we present here and is initialized from the previous model runs (Nickovic et al. 2001). A third dust prediction system, SKIRON, is from the University of Athens (http://forecast.uoa.gr/forecastnew.html) and is also based on the Eta system and AS-MEDUSE initialization (Nickovic et al. 1997). There are additional similar dust models operating in Egypt and Denmark.

2. The model

a. Data and the model

The TAU version of the Eta Model uses a horizontal resolution of 50 km and has 32 vertical levels. The model is initialized with the NCEP analysis and the lateral boundary data are updated every 6 h, from the operational forecasts by the NCEP global model. The data are presently available for retrieval with horizontal resolution of 1.25° at 10 isobaric surfaces (1000, 850, 700, 600, 500, 400, 300, 200, 150, and 100 hPa) about 5 h after the corresponding observation time. The expanded area of the TAU Eta Model forecast includes the tropical North Atlantic Ocean, North Africa, the Middle East, and the Arabian Peninsula. Only the eastern part of the model region is shown in the figures presented here. The runs start with 1200 UTC data and the forecasts are presently performed for periods up to 48 h (Krichak et al. 1999b). The physical package of the model includes blocks for dust initialization, transport, and wet/dry deposition (Nickovic et al. 1997), in addition to the other Eta physical parameterization schemes. The latter include large-scale (stable) and convective precipitation, long- and shortwave radiation, a land surface model, and viscous sublayer models (Mesinger et al. 1988; Mesinger 1996). Further details on the model numerics and physics can be found in appendix A. The distribution of desert dust sources is specified according to the Olson World Ecosystem (OWE) dataset (Olson et al. 1995), which contains 59 classes of vegetation with $10' \times 10'$ resolution. In the present experiments a single aerosol size (5-μm diameter) was assumed, as in the MEDUSE project. Alpert and Ganor (2001) show that 2–2.5-μm radius is the most dominant aerosol size in a Saharan dust intrusion over Israel. The single-size aerosol is, however, a major shortcoming of the current system and we are currently experimenting with a number of aerosol sizes.

b. Modification introduced in the TAU dust prediction system

The TAU Eta dust and weather prediction system uses a new technique for determination of the three-dimensional initial distribution of the mineral dust concentration. The technique is based on the TOMS aerosol index measurements and is described in the next section.

The dust modeling system includes an optimized digital classification of dust sources as follows. Using the long record of TOMS aerosol products, Prospero et al. (2001) showed that the aerosol index maxima form a persistent pattern over the years and can often be associated with topographic depressions. These depressions are usually dry lakes (called playa), which formed during the late Pleistocene or Holocene. These former lakes have accumulated a deep layer of sediments composed of fine clay particles, which are now easily eroded by winds. Based on this study, Ginoux et al. (2001) have developed a methodology to define the dust sources with a continuous function based on topography and vegetation. For this study, the source function has been adapted for our higher resolution model using global datasets with $10'$ by $10'$ grid.

3. Dust initialization

A new approach for determination of the 3D distribution of the dust concentration has been developed. It is based on the following considerations. It is well known (see, e.g., Nickovic et al. 1997) that one of the main problems associated with dust model prediction is the lack of regular dust observations. Several possibilities for solving the problem exist.

a. Zero dust initialization

The model is initialized with zero dust and is allowed to generate and distribute the dust. The main shortcoming here is the necessity to let the model generate, build up, and transport its own dust while we know that lifetime of some dust plumes can easily exceed a few days or even weeks (Prospero and Nees 1986). Hence, for short-range dust predictions, up to 48 h, this is a serious problem, as illustrated later in the skill scores (Table 1). In brevity, this approach will be entitled ORDINARY.

b. Employing previous dust model output

This is based on the assumption that the dust concentrations produced by the model during the first 12–24-h time period may be a reasonable substitution for the absent objective analysis data for the dust concentrations (Nickovic and Dobricic 1996). Hence, 3D dust concentrations computed in the previous runs are employed at the initialization time for the current forecast. Though the method is often quite successful in describing the initial state for the forecast [as in the MEDUSE project; e.g., Nickovic et al. (1997)], its main shortcoming is clear; when the dust forecast fails, its 3D dust distribution serves as a wrong input for the following run. In brevity, this approach will be entitled AS-MEDUSE.

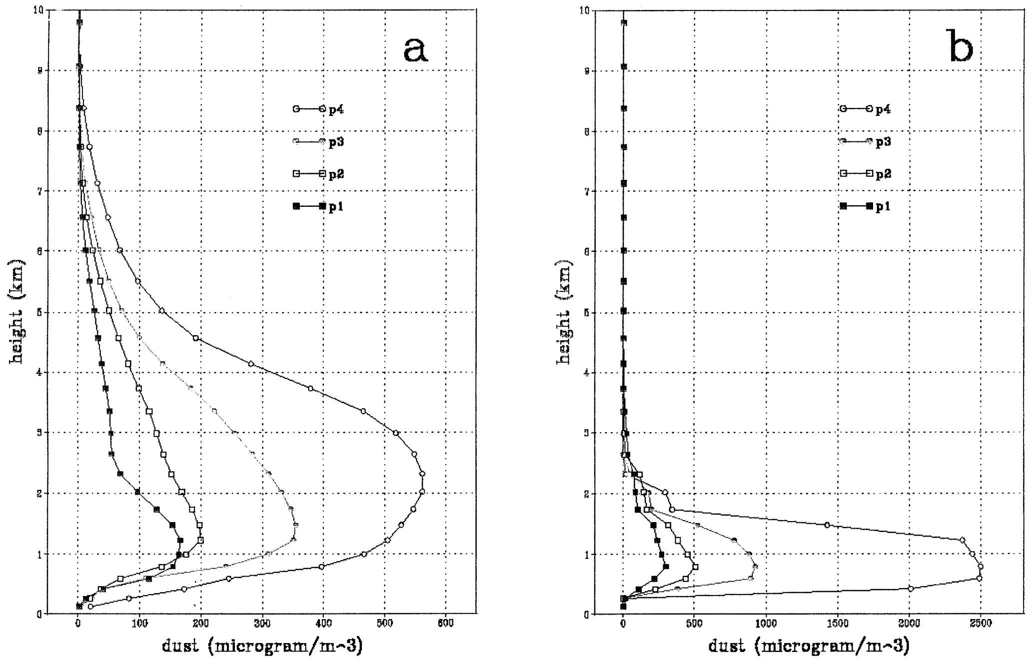

FIG. 1. The model-calculated dust profiles for (a) the Mediterranean and (b) the Sahara regions, based on a number of simulations; notice the significant difference in the scale of the dust concentrations in both regions. The four profiles correspond to the average model output profiles at the four respective TOMS AI domains: 0.7–1.1 (p1), 1.1–1.5 (p2), 1.5–1.9 (p3), and >1.9 (p4).

c. Employing TOMS Aerosol Index data

As shown by Herman et al. (1997) and Hsu et al. (1999), the TOMS aerosol index (AI) describes quite well the approximate geographic distribution of vertically integrated amounts of absorbing aerosols over the earth once a day. (A minimum value of AI = 0.7 was chosen since weak TOMS AI signals show much noise; experiments with a value of AI = 1.1 were also performed.) However, there is a need to translate the AI into total column dust loading and distribute it vertically for the initialization of the dust model as described next.

To determine the vertical distribution of the dust we have studied the climatology of vertical dust profiles accumulated at Tel Aviv University over two different regions from our semioperational runs using the first approach. The resulting profiles (Fig. 1) were compared to earlier sparse data as from the Lidar In-space Technology Experiment (LITE; http://asd-www.larc.nasa.gov/ASDhomepage.html) and other observational experiments over Africa and the Atlantic Ocean, which show dust layers in the boundary layer or above (Karyampudi et al. 1999; Karyampudi 1986). Over the Mediterranean, however, lidar measurements in Greece (at Thessaloniki and OHP) suggest that the transported dust is multilayered (Hammonou et al. 1999), with several distinct layers at altitudes between 1.5 and 5 km. Another more recent lidar study (from Crete) analyzing 21 days in May 1999 suggests that there are periods of strong dust perturbations above the boundary layer that may extend up to the altitude of 10 km and that may last for several days (Gobbi et al. 2000).

Figures 1a and 1b show the resulting dust profiles for the Mediterranean and the Sahara regions, respectively; notice the significant difference in the scale of the dust concentrations in both regions. The four profiles correspond to the average model output profiles at the four respective AI domains of 0.7–1.1 (p1), 1.1–1.5 (p2), 1.5–1.9 (p3), and 1.9+ (p4). The relation between AI and the dust loading (DL) in the model was based on the approximation 0.5 AI ≅ DI (explained in appendix B). Given this relationship and the four profiles for each region the initialization procedure is as follows: The TOMS AI at a specific point is classified to its pertinent AI domain and to its region. For instance, AI = 1.6 over the Mediterranean will be assigned the AI domain 3 and the Mediterranean region. Hence, it will be assigned the profile p3 (Fig. 1a). Now, a continuity correction factor of 1.6/1.7 is applied since the profile (p3, Fig. 1a) is assumed to exactly fit the central value of its AI domain, that is, 1.7. In this way, the smoothed TOMS AI map is transformed into a smoothed profile field throughout the four AI domains. However, in the boundary between the Sahara and the Mediterranean profiles, such a discontinuity correction was not yet applied for the cases where the same plume crosses this boundary. This can be partly justified by the relatively fast adjustment in the model as experienced in our zero-dust (ORDINARY runs; see the next section) experi-

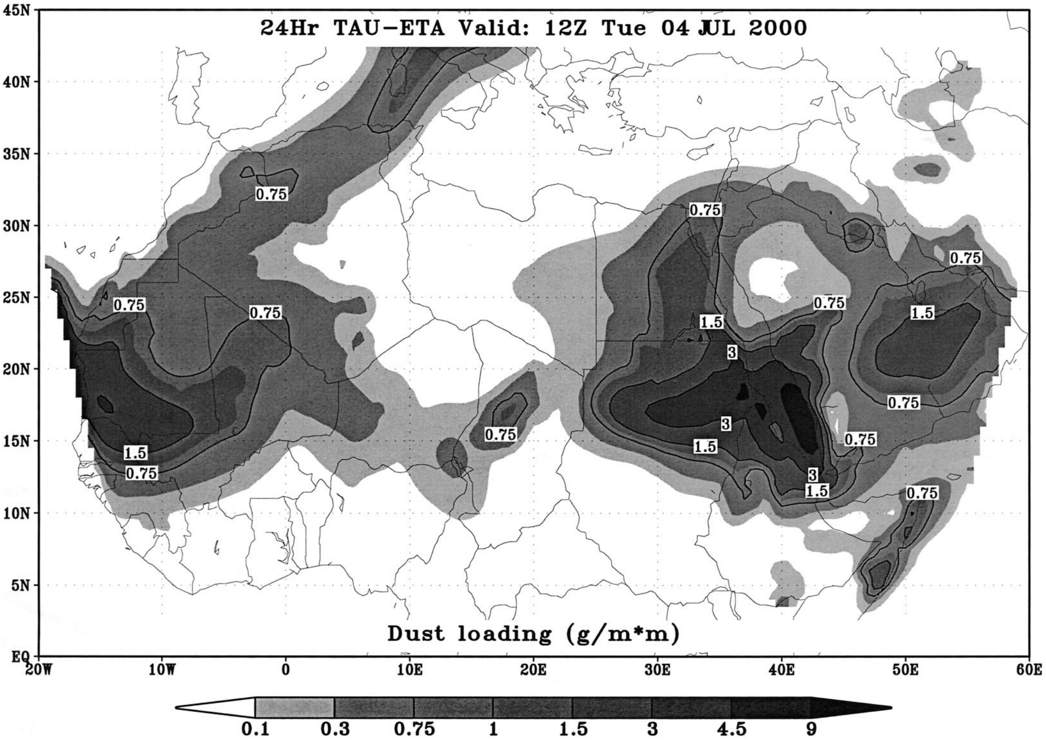

FIG. 2. The 24-h dust prediction at 1200 UTC 4 Jul 2000 over the Mediterranean and North Africa. The variable is the dust loading (g m^{-2}) shown in gray shading according to the value in the bar below. The forecast started at 1200 UTC 3 Jul 2000. Initialization with TOMS-INIT.

ments in which it was found that a few hours are required for the model to build its approximate dust mass loading in many regions. Incorporation of a smoothing algorithm between the two regions is planned.

As expected, over the Sahara the dust maximum concentration is often near the surface at altitudes below about 1 km (Fig. 1b; Karyampudi 1986; Karyampudi et al. 1999). Over the Mediterranean Sea, however, large-scale vertical motions and intensive cyclonic activity frequently destroy the boundary layer inversion layer and transport large quantities of the dust into the lower troposphere (see Fig. 1a). Over the Atlantic Ocean the variation of the thickness of the marine inversion layer largely determines the height of the maximum dust concentration. In the forthcoming experiments only profiles from two regions, that is, the Sahara and the Mediterranean, were employed (Fig. 1). For the sake of brevity, this approach will be entitled TOMS-INIT.

The next section describes the prediction for the dust case of 4 July. The July case was chosen here because it is an exceptional event for which the prediction system has performed reasonably well. Then, results of the model verification for a number of operational runs are presented.

4. The dust case of 4 July

Figure 2 shows the 24-h dust prediction for 1200 UTC 4 July 2000. The synoptic system that prevailed over the Mid-East on 4 July (like on nearly all summer days from mid-June to mid-September) was a surface Persian trough toward the Eastern Mediterranean along with a surface subtropical ridge from the Azores all the way through North Africa, the Southern Mediterranean, and toward Israel (Alpert et al. 1990a). The variable in Fig. 2 is the dust loading (g m^{-2}), and the model prediction clearly shows a narrow dust plume penetrating Israel (30°N, 33°E) from the south over the Eastern Mediterranean with a maximum value of about 1 g m^{-2}. Another northward intrusion of the Sahara dust plume can be noticed over the Western Mediterranean toward central Italy (38°–42°N, 10°E). There seems to be some similarity with another case of a deep dust intrusion in the Western Mediterranean—to Italy—on 30 December 1985, which was studied in detail by Alpert and Ganor (1993). For verification, Fig. 3 shows the TOMS aerosol index for 4 July 2000, at about 0900–1000 UTC. Both intrusions over Italy and Israel are noticeable in the TOMS AI as well. Of particular interest is the eastwards bending of the dust plume (maximum loading) over the Eastern Mediterranean, which is also predicted by the model dust loading, though weaker than observed. It could be that our threshold of AI = 0.7 for TOMS-INIT may be partially responsible for the weaker dust plume in the model prediction. Figure 4 shows the 48-h prediction for 4 July, which includes indications of the two observed dust plume intrusions, though much weaker than observed.

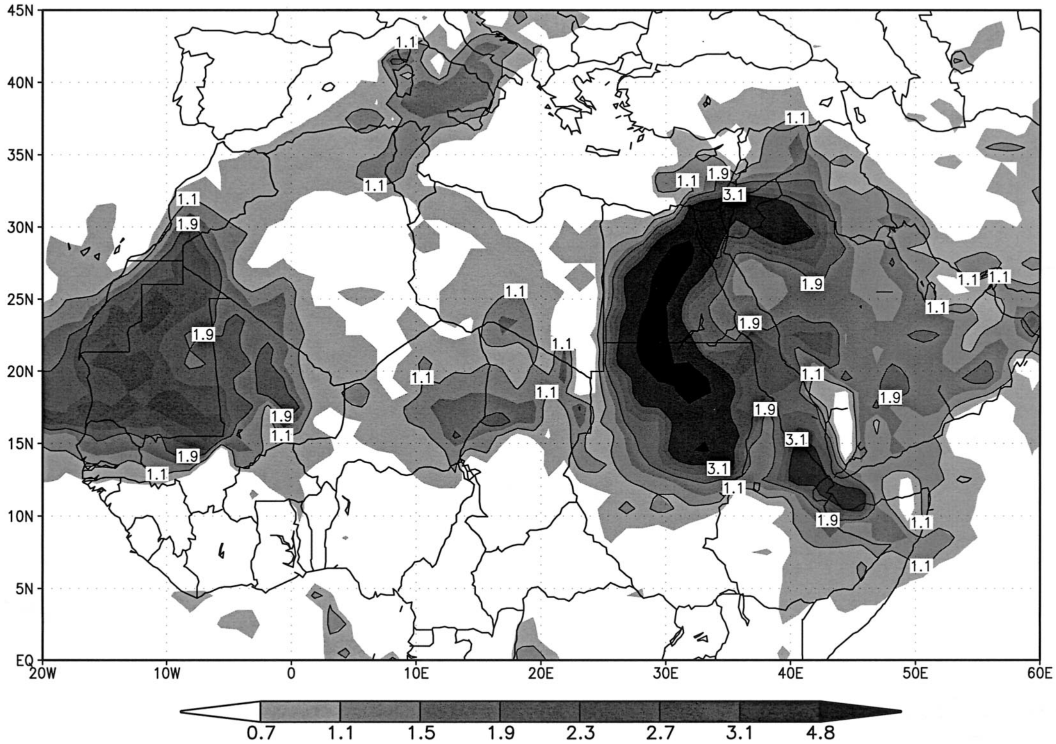

FIG. 3. The 4 Jul 2000 TOMS AI map for the Mediterranean and North Africa. Time (which is *not* fully synoptic) is about 0900–1000 UTC; see Herman et al. (1997).

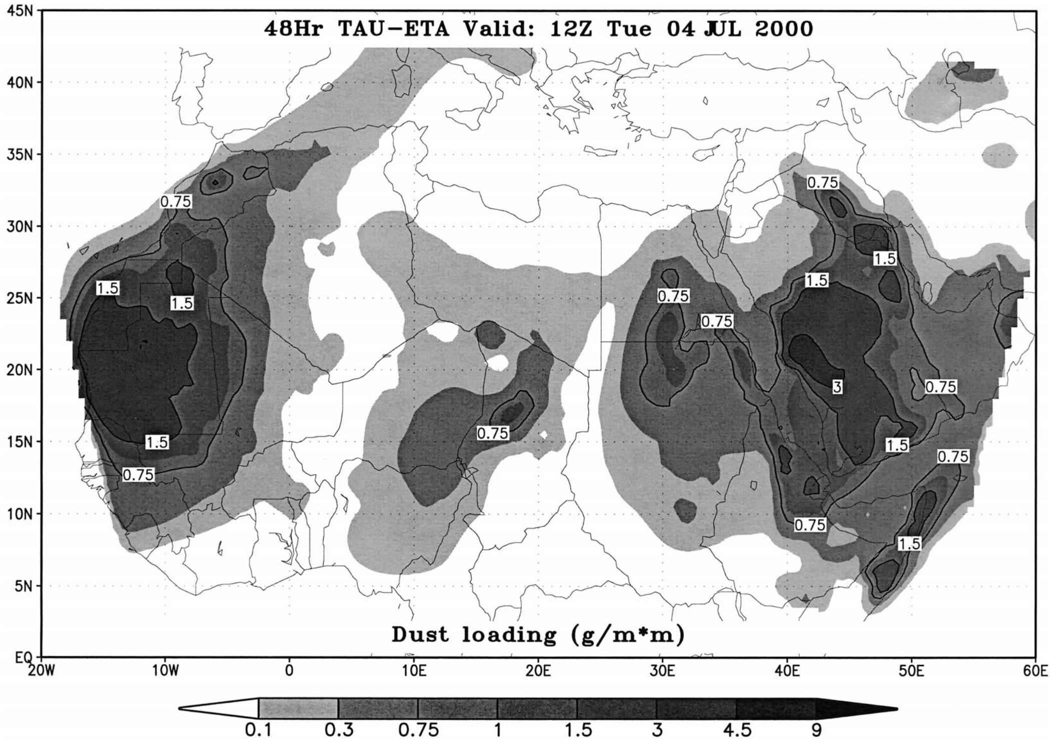

FIG. 4. As in Fig. 2 but for the 48-h dust prediction at 1200 UTC 4 Jul 2000. The forecast started at 1200 UTC, 2 Jul 2000.

The large drop in the quality of the forecast from 24- to 48-h prediction (Figs. 2 and 4 as compared to Fig. 3) may be an indication to the impact of the improved initialization with TOMS data. The quantitative contribution of the TOMS initialization to the prediction skill is illustrated in the next section. It should also be noted that the sensitivity of the TOMS AI to the altitude of the dust plume may have played a role in both artificially enhancing the dust in the initialization (since the dust was at higher altitudes as discussed later) as well as in the verification against TOMS AI. However, the Aerosol Robotic Network (AERONET) measurements discussed next do indicate a significant dust plume with an aerosol optical thickness (AOT) of about 1.4.

Summer outbreaks of dust over the Eastern Mediterranean are relatively rare. This area gets frequent intrusions of dust in spring (Alpert and Ziv 1989; Alpert et al. 2000; Moulin et al. 1997) with a secondary maximum in the autumn (Ganor 1994). The dynamical system that transports the dust is primarily the Sharav cyclone, which is also called the Saharan depression, generated in the lee of the Atlas Mountains (Egger et al. 1995) and moving along the North African coast eastward (Alpert et al. 1990b). The Sharav cyclone is clearly not the associated synoptic system in summer. In the present summer case, inspection of the route of the dust plume suggests that the strong dry convection over the Sahara source regions has lifted the dust to high-enough altitude (say above 700 hPa), which would allow the upper-level southwesterlies to transport the dust northeastward into the Eastern Mediterranean.

Figure 5 shows the AERONET AOT measured in Sede-Boker, Southern Israel (at about 31°N, 34°E), during the whole month of July 2000. Values are for wavelength of 500 nm. All 4 July measurements show AOT well exceeding 1, reaching a maximum of 1.5, and most of the time being above 1.3. The maximum fits well the time of the TOMS imagery (Fig. 3) when a plume with AI > 2.7 is located over Southern Israel and Sede-Boker. Such events are rare in summer (e.g., Ganor 1994); we examined the AERONET AOT in Sede-Boker for July 1996, 1998, 1999, and 2000 and the 4 July event is clearly the strongest. Nearly all days show AOT values below 0.4. The second strongest dust event was found on 28 July 1996, when a peak of 1.4 was reached, but most of the day the values were below AOT $= 0.6$. It seems that these rare summer events are associated with high-altitude transport of dust above the planetary boundary layer (PBL), probably above or near 500 hPa. The low-level semipermanent monsoonal Persian trough over the Eastern Mediterranean and the associated strong northwesterly Etesian winds from Greece to Israel that dominate the area would not allow low-level transport from North Africa (Alpert et al. 1990a).

Another case study of an exceptionally severe duststorm on 14–17 March 1998 was also recently investigated (Alpert and Ganor 2001) and successfully simulated by our dust prediction even without the TOMS initialization (Tsidulko et al. 2002). Our dust Web site (http://earth.nasa.proj.ac.il/dust/) includes past predictions since July 2000, and routine verification shows that the model is quite successful through all seasons.

5. Model verification

a. Verification against TOMS AI

Table 1 summarizes the scores for four different verification methods, all against the TOMS AI data: threat score, total mass correlation, difference in the dust plume orientation, and the average distance between centers of mass. The latter was calculated by weighting each model grid point or TOMS pixel according to the distance from the mass center. The orientation of the plume was determined by fitting the best ellipse to both the model dust loading and to the TOMS picture. The fit between the model dust loading and the TOMS AI values was based on subjective comparison of a large number of pictures. Also, as discussed earlier (and in appendix B), the approximate relation between dust loading and TOMS AI is $0.5\text{AI} \cong \text{DL}$, where DL stands for the dust loading. Hence, the thresholds for calculating the threat scores are AI $= 1.5$ for TOMS, corresponding to DL $= 0.75$ g m^{-2}. A comparison between TOMS AI and surface dust concentrations was recently also attempted by Alpert and Ganor (2001). But there the surface measurement is clearly not a column-integrated measure of dust, as is the case with the DL.

Four different experiments were compared. 1) ORDINARY—the model initializes with zero dust; 2) AS-MEDUSE—the Model initializes with 3D dust distributions from a previous (24 h) run. This procedure was adopted from the MEDUSE project (Nickovic et al. 1997). 3) GINOUX-SOURCES—the Dust sources are taken from the Ginoux et al. (2001) method and dust initialization as in AS-MEDUSE. 4) TOMS-INIT—the model initialization is based on TOMS as described earlier (section 2c) and the Ginoux et al. dust sources. The tests for the TOMS-INIT runs were for two months, while the other experiments were run for one month only. Results of Table 1 clearly show that the TOMS initialization (exp 4) has a significant positive impact on all the scores. In particular, the threat score that is a tough measure for any atmospheric field reaches mean values higher than 0.4 for the significant thresholds of AI $= 1.5$. For comparison, threat scores achieved in precipitation forecasts are in general well below 0.4 for rainfall thresholds above 0.1 in. (WMO 1993). In a more recent comparison of eight global models and the superensemble (run at the Florida State University) for the year 2000, the threat scores for rainfall above 10 mm day^{-1} are still, in general, well below 0.4 (http://estero.met.fsu.edu:5080/rtnwp/).

The other test scores have been especially developed for the present problem of the forecast of dust palls and plumes. Specific clearly identifiable plumes were chosen

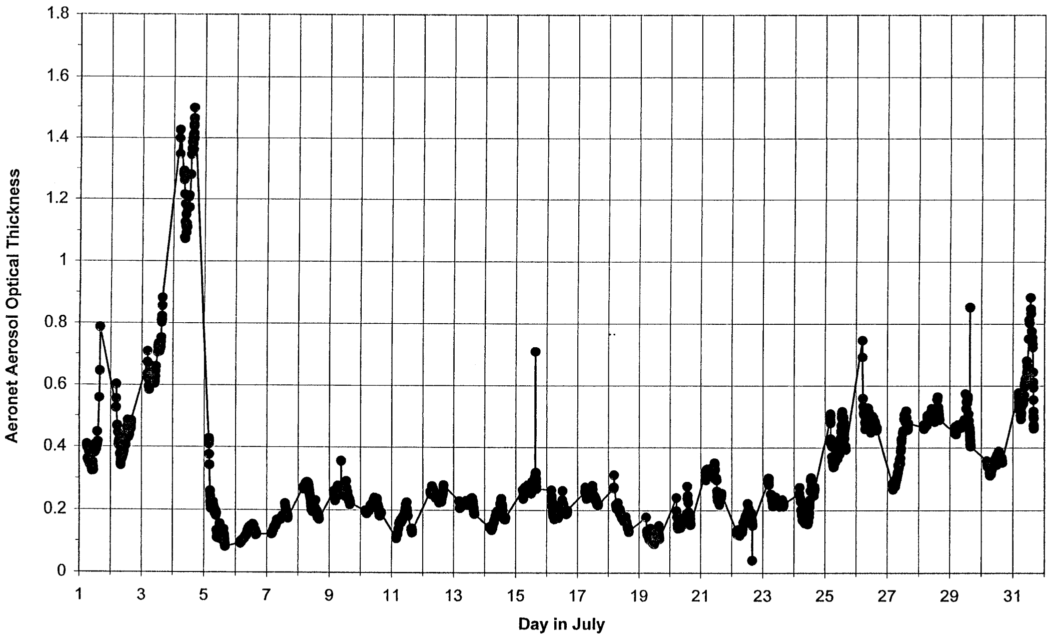

FIG. 5. The AERONET AOT, measured in Sede-Boker, Southern Israel (at about 31°N, 34°E) during Jul 2000. Values are for wavelength of 500 nm.

from the forecasts and the appropriate parts from the TOMS imagery were selected. A best-fit ellipse was calculated objectively through the formulation of the tensor of inertia. By diagonalization of the inertia tensor and the orthogonal rotation, the tilt angle of the ellipse was calculated. In this way, evaluation of a dust plume's orientation was performed, and the direction of the major axis of the ellipse is calculated. The gravity center of mass was based upon that calculation for both the model DL and the TOMS-AI data. The total mass is calculated by integration over the area of the plumes. The average distance between the centers of mass of the two corresponding plumes—one in the TOMS map and one in the forecast map—is calculated from the model DL and the TOMS image brightness.

The results are summarized in Table 1 and show equal tendencies for the different scores. A particular advantage for MEIDEX, and the topic of this paper, is the result that only in the TOMS-INIT experiment does the average distance between the predicted and the TOMS-observed mass centers drop below 200 km, as was operationally required.

b. Verification against surface measurements

Figures 6a and 6b present the model 24- and 48-h dust loading, respectively, in Tel Aviv versus the measured dust concentrations for the month of April 2001. Surface data are from the Electrical Company at the Yad LaBanim station, and the Department of Geography, Tel Aviv Uni-

TABLE 1. Summary of the scores for four different verification methods all against the TOMS AI data: threat score, total mass correlation, difference in the dust plume orientation (°) and average distance between centers of mass (km). Four different run experiments were compared: 1) ORDINARY—the model initializes with zero dust. 2) AS_MEDUSE—model initializes with 3D dust distributions from a previous (24 h) run. 3) GINOUX-SOURCES—dust sources are taken from the Ginoux et al. method (2001). 4) TOMS_INIT—model initializations based on TOMS as described earlier and the Ginoux et al. dust sources. The thresholds for calculating the threat scores are AI $>$ 1.5 for TOMS and above 0.75 g m^{-2} for the Eta Model dust loading. The same thresholds were taken for the four experiments. The tests for the TOMS-INIT runs were in Mar and Jun 2000. All other experiments were in Mar 1999 before the TOMS-INIT approach was applied. Number in parentheses count the verified forecasts in each case. The TOMS-INIT predictions started at 1200 UTC (close to the time of the TOMS data) and therefore verification times are for 24 h (marked by one asterisk) and 48 h (marked by two asterisks), instead of 12 and 36 h, respectively, as in the other runs.

		Mean threat score		Total mass correlation		Difference dust plume orientation (°)		Avg distance between centers of mass (km)	
No.	Expt	12 h	36 h	12 h	36 h	12 h	36 h	12 h	36 h
1	ORDINARY	0.22 (18)	0.20 (17)	0.04 (20)	0.49 (20)	23.0 (12)	17.1 (12)	448.4 (12)	355.4 (12)
2	AS_MEDUSE	0.25 (13)	0.17 (11)	0.86 (15)	0.91 (14)	18.8 (14)	15.6 (13)	485.7 (14)	500.3 (13)
3	GINOUX_SOURCES	0.28 (13)	0.22 (13)	0.72 (16)	0.65 (16)	13.9 (14)	14.0 (14)	351.7 (14)	351.6 (14)
4	TOMS_INIT	0.47 (27)*	0.43 (27)**	0.77 (27)*	0.72 (27)**	12.0 (36)*	13.3 (30)**	193.2 (36)*	175.0 (30)**

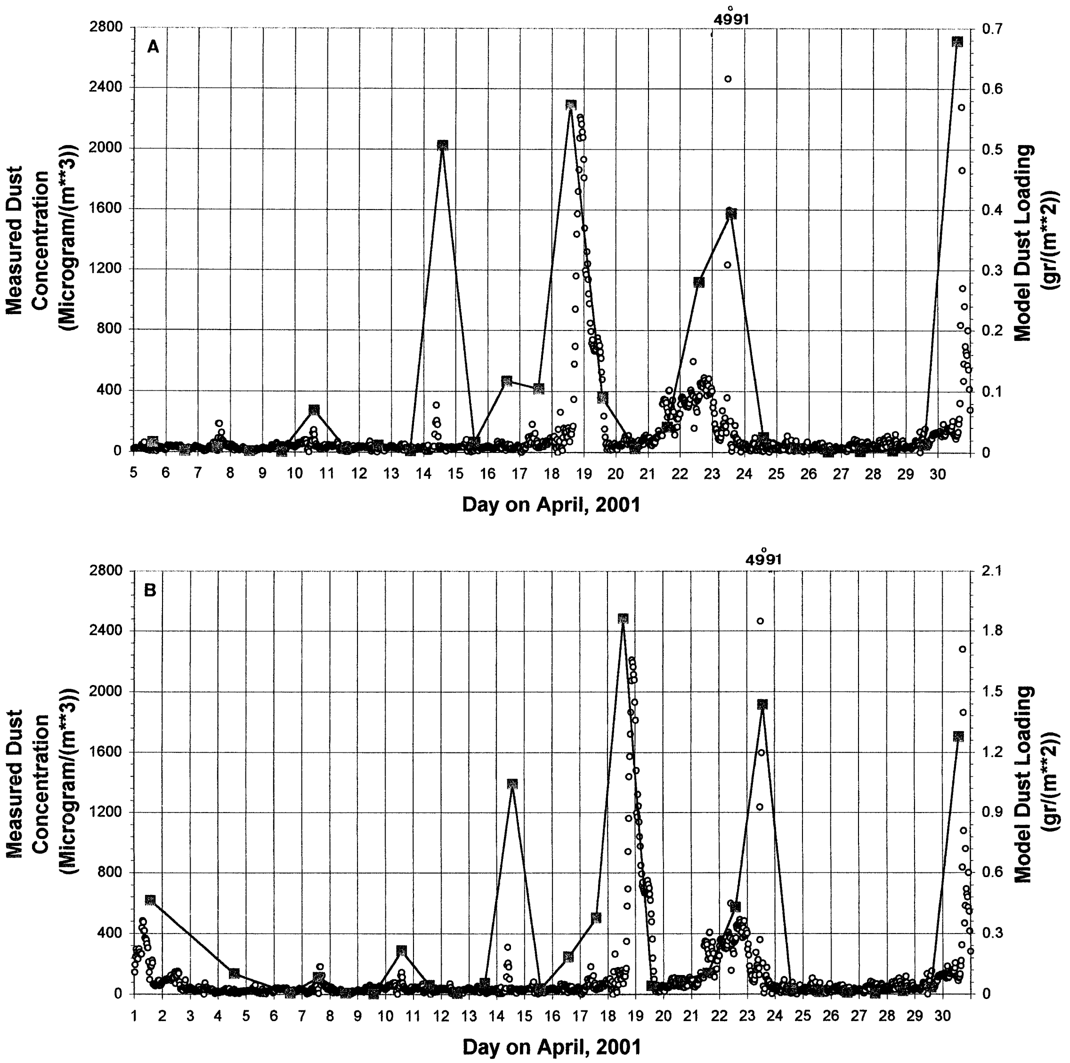

FIG. 6. The model (a) 24- and (b) 48-h dust loading (squares) in Tel Aviv vs the measured dust concentrations (circles) for Apr 2001. Surface data are from the Electrical Company at station Yad LaBanim and the Department of Geography, Tel Aviv University. One measurement on 23 Apr reached 4991 μg m^{-3}, exceeding the scale of 2800 μg m^{-3}, and is indicated with its value at the pertinent time. All are TOMS-INIT runs. For performing the correlations the Electrical Company daily 0700–1700 data were averaged (half-hourly point data). For the model, the noontime (1200 UTC) forcast was spatially averaged over a box of 200 km $\times$ 200 km around the station.

versity. All are TOMS-INIT runs. The correlation coefficients between the DL and the surface concentrations are 0.69 for both the 24- and 48-h runs, based on 27 predictions. For performing the correlations, the Electrical Company daily 0700–1700 data were averaged (half-hourly point data). For the model, the noontime (1200 UTC) forecast was spatially averaged over a box of 200 km $\times$ 200 km around the station. Figure 6b illustrates that the model was successful in predicting all seven dust events (exceeding a threshold of about 100 μg m^{-3}). It should be noted that, in contrast to expectations, the correlations with model surface concentrations were lower, that is, 0.48 (26) and 0.38 (27), where the number in parentheses stands for the number of predictions in each case. This requires further investigation and may be the result of a single-size dust aerosol. AS-MEDUSE experiments were only available for half of the month of March 1999. Hence, a similar examination of the correlation with Tel Aviv surface observations (at station Shikun Lamed, Tel Aviv) has yielded lower correlations, that is, 0.48 (13) and 0.42 (12) for 12 and 36 h, respectively. This further supports the advantage of TOMS-INIT runs. The significance levels for the TOMS-INIT correlations were higher than 95%, while for the AS-MEDUSE runs the levels of significance were above 95% and 90%, respectively. The AS-MEDUSE comparisons are less significant due to both lower correlations and a reduced number of events.

It should be noted that in the present application the cloud contamination on the TOMS AI has not yet been addressed (Torres et al. 1998). Corrections for artificially high TOMS AI due to cloudiness below dust layers are necessary and this effect may be responsible for the overestimation of some of the predicted dust peaks in Figs. 6a and 6b. Fortunately, the Sahara has generally small amounts of clouds, which reduces this negative effect.

6. Summary

This paper presents results of some optimization efforts of a dust prediction system, developed earlier at the University of Athens, within the framework of the MEDUSE project. The work was performed in order to support the Israeli–American MEIDEX project. These enhancements include development of a new dust initialization approach using TOMS aerosol index (AI) data and improved specification of the dust sources. The improved skill of the model against the TOMS AI measurements was tested over two periods in March and June 2000 using four different scores. The scores are for four different verification methods, all against the TOMS AI data: threat score, total mass correlation, difference in the dust plume orientation, and the average distance between centers of mass. Four sets of experiments that differ by the dust initialization and the dust sources determination were compared: 1) ORDINARY—the model initializes with zero dust, 2) AS-MEDUSE—model initializes with 3D dust distributions from a previous (24 h) run, 3) GINOUX-SOURCES—dust sources are according to the Ginoux et al. method and dust initialization as in AS-MEDUSE, and 4) TOMS-INIT—model initialization based on TOMS and Ginoux et al. dust sources. Results tested against TOMS AI by the aforementioned conventional and novel methods specific to dust forecasting clearly show that the TOMS initialization (exp 4) has a significant positive impact on all the scores. In particular, the threat score that is a tough measure for any atmospheric field reaches values higher than 0.4. Also, the average distance between the predicted and the TOMS-observed mass centers drops below 200 km, as was operationally required, in the TOMS-INIT runs only.

It should be noted that in the present application the effect of cloud contamination on the TOMS AI has not yet been addressed. Correction for artificially high TOMS AI due to cloudiness below dust layers is necessary. Fortunately, the Sahara generally has a small amount of clouds, which reduces this negative effect in our region as long as the dust initialization is mostly over cloud-free regions. Another problem related to dust initialization cloudiness is the lack of TOMS AI data in cloudy regions. One way to address this problem is by using a combined initialization of TOMS AI and previous model dust output.

This project is on going and includes further comparisons with AERONET, surface dust measurements, sun-photometer data, Moderate Resolution Imaging Spectroradiometer (MODIS), and Sea-viewing Wide Field-of-view Sensor (SeaWiFS) data as well as other dust predictions systems.

Acknowledgments. Thanks are given for the support to S. Krichak and M. Tsidulko from the EU Icarus Project. Thanks are given to F. Mesinger, D. Jovic, and C. Bruyere for help in the adaptation of the NCEP Eta atmospheric model for TAU. Special thanks for the active aid from the University of Athens group: A. Papadopoulos, O. Kakaliagou, and G. Kallos, are given. The system has been earlier developed at University of Athens within the MEDUSE project framework, funded by DG-XII of the European Union (EU) and the Greek government: EU project SKIRON. Further significant improvements were performed within the framework of the BSF Grant-97-00448 and MEIDEX projects with financial MEIDEX support to M. Tsidulko, H. Shafir, and E. Klodz. The Web page was created by R. Parparov with the help of the EOSDIS Node in Israel (ISA-MEIDA). Thanks are given to Paul Ginoux for advice and for running the program of dust sources with higher resolution for our region. Thanks are given to A. Shtivelman for help with Fig. 1.

APPENDIX A

Characteristics of the TAU Weather and Dust Prediction Eta Atmospheric Model

a. Dynamics and numerics

- Hydrostatic NCEP Eta sigma-eta vertical coordinate model (Mesinger 1997)
- Model domain: 0°–50°N, 50°W–50°E; number of vertical levels: 32; horizontal spacing: 0.5°
- Arakawa E grid in the horizontal, vertical Eta (step-like) silhouette topography (Mesinger 1997)
- Conservation of finite-difference analogs of chosen integral constrains of the continuous atmosphere (Arakawa 1966)
- Minimization of spurious departures from the physical system, computational modes, and false instabilities
- Horizontal advection of passive substances (including dust concentration): conservative positive-definite scheme (Janjić 1994)

b. Dust parameterization

- Dust prediction (mobilization, transport, wet/dry deposition) (Nickovic et al. 1997, 2001)
- Optimized determination of the dust sources employing the Ginoux et al. (2001) method (http://cdiac.esd.ornl.gov/ftp/ndp017/ndp017.txt)

c. Physics

- No aerosol radiative feedback is included

- Land-surface scheme (Chen et al. 1997)
- According to Monin–Obukhov similarity theory with the use of Mellor and Yamada (1982); level-2 model with the stability functions determined as in Łobocki (1993) for water and Paulson (1970) for land; viscous sublayer approach is adapted over land, (Zilitinkevich 1995), and over water (Janjić 1994)
- Cumulus parameterization: Betts–Miller–Janjić deep and shallow moist convection scheme (Betts 1986; Janjić 1994)
- Radiation (Lacis and Hansen 1974; Fels and Schwartzkopf 1975)

APPENDIX B

Relation between TOMS AI and Dust Loading (DL)

Following Torres et al. (1998), to a first approximation the AI can be assumed (ignoring the viewing geometry factor) as a function of the altitude z of the gravity center of the dust plume, the optical depth τ, and the single-scattering albedo ω of the aerosol. Hence,

$$\mathrm{AI} \cong f(z, \tau, \omega). \tag{B1}$$

Assuming ω = constant, for Saharan mineral dust and neglecting the effects of changing geometry angles, one can further assume (Hsu et al. 1999)

$$\mathrm{AI} \cong f(z, \tau). \tag{B2}$$

We do not know the relation with z, and it could be as important in determining AI as is the optical thickness. In our preliminary investigation we will assume that

$$\mathrm{AI} \cong 4\tau. \tag{B3}$$

Hsu et al. (1999) showed the existence of a linear relationship using ground-based sun-photometer data for specific sites. Although the constant varies according to place and season here we assume a constant factor.

For large particles having the same size distributions at each height, the total column mass loading DL can be written as

$$\mathrm{DL} = (2/3)\rho\tau r_e, \tag{B4}$$

where ρ is the mass density of the aerosol material and r_e is the aerosol effective radius. Substituting DL into AI expression yields

$$\mathrm{DL} \cong (1/6)\rho\mathrm{AI}r_e. \tag{B5}$$

Hence, for $\rho = 2.3$ g cm^{-3}, $r_e = 1$ μm, one gets

$$\mathrm{DL}(\mathrm{g\ m^{-2}}) \cong 0.5\mathrm{AI} \tag{B6}$$

REFERENCES

Alpert, P., and B. Ziv, 1989: The Sharav cyclone—Observations and some theoretical considerations. *J. Geophys. Res.,* **94,** 18 495–18 514.

——, and E. Ganor, 1993: A jet-stream associated heavy dust storm in the western Mediterranean. *J. Geophys. Res.,* **98,** 7339–7349.

——, and ——, 2001: Sahara mineral dust measurements from TOMS—Comparison to surface observations over the Middle-East for the extreme dust storm, 14–17 March 1998. *J. Geophys. Res.,* **106** (D16), 18 275–18 286.

——, R. Abramsky, and B. U. Neeman, 1990a: The prevailing summer synoptic system in Israel—Subtropical high, not Persian trough. *Isr. J. Earth Sci.,* **39,** 93–102.

——, B. U. Neeman, and Y. Shay-El, 1990b: Intermonthly variability of cyclone tracks in the Mediterranean. *J. Climate,* **3,** 1474–1478.

——, J. Herman, Y. J. Kaufman, and I. Carmona, 2000: Response of the climatic temperature to dust forcing, inferred from TOMS Aerosol Index and the NASA assimilation model. *J. Atmos. Res.,* **53,** 3–14.

Arakawa, A., 1966: Computational design for long-term numerical integration of the equations of fluid motion: 2 dimensional incompressible flow. Part. I. *J. Comput. Phys.,* **1,** 119–143.

Betts, A., 1986: A new convective adjustment scheme. Part E—Observational and theoretical basis. *Quart. J. Roy. Meteor. Soc.,* **112,** 677–691.

Chen, F., Z. Janjic, and K. Mitchell, 1997: Impact of atmospheric surface-layer parameterizations in the new land-surface scheme of the NCEP mesoscale Eta Model. *Bound.-Layer Meteor.,* **85,** 391–421.

Christensen, J. H., 1997: The Danish Eulerian hemispheric model—A three-dimensional air pollution model used for the Arctic. *Atmos. Environ.,* **31,** 4169–4191.

Egger, J., P. Alpert, A. Tafferner, and B. Ziv, 1995: Numerical experiments on the genesis of Sharav cyclones; Part I: Idealized simulations. *Tellus,* **47A,** 162–174.

Fels, S. H., and N. D. Schwartzkopf, 1975: The simplified exchange approximation: A new method for radiative transfer calculations. *J. Atmos. Sci.,* **32,** 1475–1488.

Ganor, E., 1994: The frequency of Saharan dust episodes over Tel-Aviv, Israel. *Atmos. Environ.,* **28,** 2867–2871.

Ginoux, P., M. Chin, I. Tegen, J. Prospero, B. Holben, O. Dubovik, and S. J. Lin, 2001: Sources and distributions of dust aerosols simulated with the GOCART model. *J. Geophys. Res.,* **106,** 20 255–20 274.

Gobbi, G. P., F. Barnaba, R. Giorgi, and A. Santacasa, 2000: Altitude-resolved properties of a Saharan dust event over the Mediterranean. *Atmos. Environ.,* **34,** 5119–5127.

Hammonou, E., P. Chazette, D. Balis, F. Dulac, X. Schneider, F. Ancellet, and A. Papayannis, 1999: Characterization of the vertical structure of Saharan dust export to the Mediterranean basin. *J. Geophys. Res.,* **104,** 22 257–22 270.

Herman, J. R., P. K. Bhartia, O. Torres, C. Hsu, C. Seftor, and E. Celarier, 1997: Global distribution of UV-absorbing aerosols from Nimbus 7–TOMS data. *J. Geophys. Res.,* **102,** 16 911–16 922.

Hsu, N. C., J. R. Herman, O. Torres, B. N. Holben, D. Tanre, T. F. Eck, A. Smirnov, B. Chatenet, and F. Lavenu, 1999: Comparisons of the TOMS Aerosol Index with sun-photometer aerosol optical thickness: Results and applications. *J. Geophys. Res.,* **104,** 6269–6279.

Janjić, Z. I. 1994: The step-mountain Eta coordinate model: Further developments of the convection, viscous sublayer, and turbulence closure schemes. *Mon. Wea. Rev.,* **122,** 927–945.

Karyampudi, V. M., 1986: A numerical study of the evolution, structure and energetics of the Saharan air layer. Ph.D. thesis, The Pennsylvania State University, 287 pp.

——, and Coauthors, 1999: Validation of the Saharan dust plume conceptual model using lidar, Meteosat, and ECMWF data. *Bull. Amer. Meteor. Soc.,* **80,** 1045–1075.

Krichak, S. O., M. Tsidulko, and P. Alpert, 1999a: Application of Eta model at Tel Aviv University for weather prediction over the Eastern Mediterranean. *Research Activities in Atmospheric and Oceanic Modeling,* H. Ritchie, Ed., WMO/TD-No. 942, pg. 5.29.

——, ——, ——, A. Papadopoulos, O. Kakaliagou, and G. Kallos, 1999b: Eta weather prediction system with the aerosol production/transport/deposition at TAU. *Research Activities in Atmospheric and Oceanic Modeling,* H. Ritchie, Ed., WMO/TD-No. 942, pg. 5.27.

Lacis, A. A., and J. E. Hansen, 1974: A parameterization for the absorption of solar radiation in the earth's atmosphere. *J. Atmos. Sci.,* **31,** 118–133.

Łobocki, L., 1993: A procedure for derivation of surface-layer bulk relationships from simplified second-order closure models. *J. Appl. Meteor.,* **32,** 126–138.

Mellor, G. L., and T. Yamada, 1982: Development of a turbulence closure model for geophysical fluid problems. *Rev. Geophys. Space Phys.,* **20,** 851–875.

Mesinger, F., 1996: Improvements in quantitative precipitation forecasts with the Eta regional model at the NCEP: The 48-hour upgrade. *Bull. Amer. Meteor. Soc.,* **77,** 2637–2649.

——, 1997: Dynamics of limited area models: Formulation and numerical methods. *Meteor. Atmos. Phys.,* **63,** 3–14.

——, Z. I. Janjic, S. Nickovic, D. Gavrilov, and D. G. Deaven, 1988: The step-mountain coordinate: Model description and performance for cases of alpine lee cyclogenesis and for a case of an Appalachian redevelopment. *Mon. Wea. Rev.,* **116,** 1493–1518.

Moulin, C., C. E. Lambert, F. Dulac, and U. Dayan, 1997: Control of atmospheric export of dust from North Africa by the North Atlantic oscillation. *Nature,* **387,** 691–694.

Nickovic, S., and S. Dobricic, 1996: A model for long-range transport of desert dust. *Mon. Wea. Rev.,* **124,** 2537–2544.

——, G. Kallos, O. Kakaliagou, and D. Jovic, 1997: Aerosol production/transport/deposition processes in the Eta model: Desert cycle simulations. Preprints, *Proc. Symp. on Regional Weather Prediction on Parallel Computer Environments,* Athens, Greece, 137–145.

——, ——, A. Papadopoulous, and O. Kakaliagou, 2001: Model for prediction of desert dust cycle in the atmosphere. *J. Geophys. Res.,* in press.

Olson, J. S., J. A. Watts, and L. J. Allison, 1995: Major world ecosystem complexes ranked by carbon in live vegetation. Carbon Dioxide Information Center Rep. NDP-017, Oak Ridge National Laboratory, Oak Ridge, TN, 288 pp.

Paulson, C. A., 1970: The mathematical representation of wind speed and temperature profiles in the unstable atmospheric surface layer. *J. Appl. Meteor.,* **9,** 857–861.

Prospero, J. M., and R. T. Nees, 1986: Impact of the North African drought and El Niño on the mineral dust in the Barbados trade winds. *Nature,* **320,** 735–738.

——, P. Ginoux, O. Torres, and S. Nicholson, 2001: Environmental characterization of global sources of atmospheric soil dust derived from Nimbus-7 TOMS absorbing aerosol product. *Rev. Geophys.,* in press.

Torres, O., P. K. Bhartia, J. R. Herman, Z. Ahmad, and J. Gleason, 1998: Derivation of aerosol properties from satellite measurements of backscattered ultraviolet radiation. Theoretical basis. *J. Geophys. Res.,* **103** (D14), 17 099–17 110.

Tsidulko, M., S. O. Krichak, P. Alpert, O. Kakaliago, G. Kallos, and A. Papadopulous, 2002: Numerical study of a very intensive Eastern Mediterranean dust storm: 13–16 March 1998. *J. Geophys. Res.,* in press.

WMO, 1993: Weather prediction research programs: Numerical Weather Prediction Progress Report for 1992. NWPP Report Series, *No. 19,* WMO/TO No. 548, 214 pp.

Zilitinkevich, S. S., 1995: Non-local turbulent transport: Pollution dispersion aspects of coherent structure of convective flows. *Air Pollution Theory and Simulation,* H. Power, N. Moussiopoulos, and C. A. Brebbia, Eds., Vol. I, *Air Pollution III,* Computational Mechanics Publications, 53–60.